REGULAR PAPER

DOI: 10.1007/s40684-018-0059-9
ISSN 2288-6206 (Print) / 2198-0810 (Online)

Study on Process Monitoring of Elliptical Vibration Cutting by Utilizing Internal Data in Ultrasonic Elliptical Vibration Device

Hongjin Jung[1,#], Takehiro Hayasaka[1], and Eiji Shamoto[1]

1 Department of Aerospace Engineering, Nagoya University, Furo-cho, Chikusa-ku, Nagoya, Aichi, 464-8603, Japan
Corresponding Author / E-mail: hongjin.jung@mae.nagoya-u.ac.jp, TEL: +81-52-789-4491
ORCID: 0000-0003-4482-8005

KEYWORDS: Elliptical vibration cutting, Process monitoring, Internal data

In the present study, monitoring of elliptical vibration cutting process by utilizing internal data in the ultrasonic elliptical vibration device without external sensors such as a dynamometer and displacement sensor is investigated. The internal data utilized here is the change of excitation frequency, i.e. resonant frequency of the device, voltages applied to the piezoelectric actuators composing the device, and electric currents flowing through the actuators. These internal data change automatically in the elliptical vibration control system in order to keep a constant elliptical vibration against the change of the cutting process. Correlativity between the process and the internal data is described by using a vibration model of ultrasonic elliptical vibration cutting and verified by several experiments, i.e. planing and mirror surface finishing of hardened die steel carried out with single crystalline diamond tools. As a result, it is proved that it is possible to estimate the elements of elliptical vibration cutting process, e.g. tool wear and machining load, which are important for stable cutting in such precision machining.

Manuscript received: July 19, 2017 / Revised: October 27, 2017 / Accepted: November 25, 2017
This paper was presented at ISGMA 2017

1. Introduction

According to a recent trend toward manufacturing automation and unmanned operation of a plant, the importance of machining process monitoring has increased.[1-3] To monitor a machining process, external sensors such as a dynamometer and displacement sensor can be applied. However, it is not desirable in general machining environments since those sensors are expensive and sensitive, and there is often no space near the machining point for their installation. There are many researches about monitoring the machining process without using the conventional sensors in order to increase the reliability of manufacturing or to adaptively avoid vibration problems such as chatter during the machining. For example, when chatter vibration occurs, a loud and irritating sound can be captured by microphones. By analyzing this sound, it is possible to change cutting conditions such as spindle speed automatically and machine the material at more stable cutting conditions.[4,5] Especially, monitoring of cutting force is essential not only for realizing fully automated machining but for improving machining accuracy and efficiency, because the cutting force indicates several critical states of the machining process such as tool wear or breakage, chattering, and structural displacement which affect quality of machined products. Many researchers have investigated to realize technologies of sensor-less monitoring of cutting force. For example, there is a cutting force monitoring approach that estimates the cutting force based on current and speed of spindle motor or feed drive and a model that relates these measurements to the cutting force.[6-8] An in-process monitoring method of tool wear is also proposed which estimates the tool wear condition by investigating on the frequency components of the cutting force signal and analyzing the changes of its pattern in tool wearing process.[7] In addition, a sensor-less tool breakage monitoring approach is also investigated which estimates the tool breakage based on analysis of driver current in CNC milling machines and tool wear detection in milling based on the analysis of controlled machine internal signals from spindle and axes motor drives.[10,11]

Meanwhile, elliptical vibration cutting technology has been introduced for precision machining of dies and molds for optical parts and other precision parts. Process monitoring is important not only for automated machining but also for attended machining in such precision

machining. Sharp tools are utilized for better surface finish and higher machining accuracy, but such tools are fragile and it is difficult even for operators to monitor the sharpness of tools during machining. Note that the precision machining is preferably carried out in an enclosed environment in order to keep the machining environment unchanged. In order to overcome this problem, the authors proposed a new method for monitoring of elliptical vibration cutting process by utilizing internal data in the ultrasonic elliptical vibration device without external sensors.[12] The experimental results suggested that the internal data correlates well with the machining process, i.e., depth of cut.[12] However, the results are limited to orthogonal cutting with only a few experimental conditions, and monitoring of the depth of cut is insufficient when considering the practical usages of the ultrasonic elliptical vibration cutting. To step further into the nature, more comprehensive discussions in the elliptical vibration cutting model is described in this research. Precisely, diamond cutting of hardened die steel and mirror surface finishing are conducted which is the most practical usage of the elliptical vibration cutting. As a result, additional cutting process parameters, i.e., cutting width, average uncut chip thickness, and, tool wear, can be estimated by analyzing the change of internal data in the ultrasonic elliptical vibration device during the machining. The basic principle of the elliptical vibration cutting and its vibration model is described in Section 2. In Section 3, internal data of elliptical vibration controller and the relationship between the internal data and the elliptical vibration model are explained. Several experimental verifications are carried out in Section 4 where the experiment and data analysis methods are also explained. In Section 5, the results of experiments and discussions are described. Conclusions of the paper will follow in Section 6.

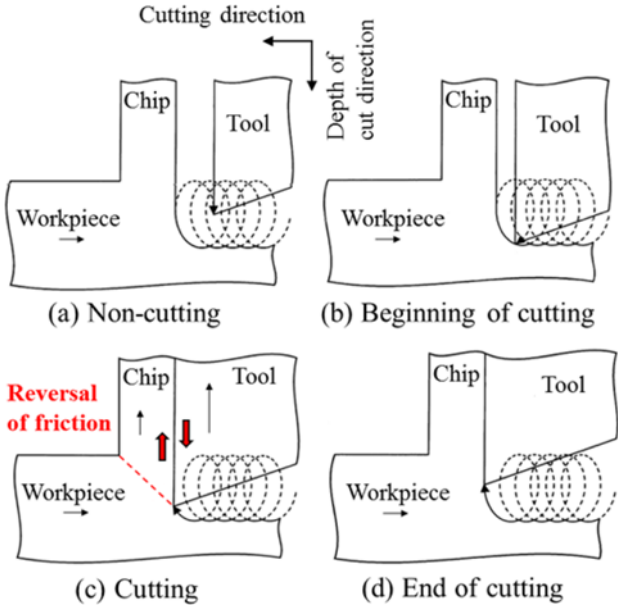

Fig. 1 Ultrasonic elliptical vibration cutting process[13] (Adapted from Ref. 13 with permission)

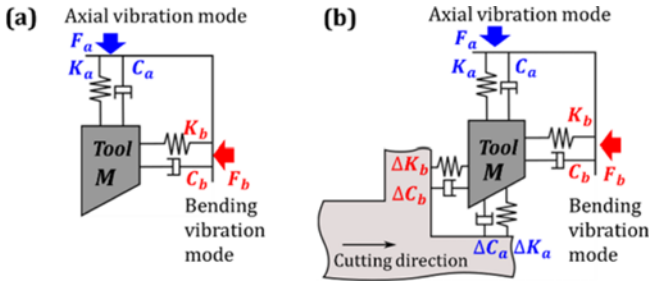

Fig. 2 Model of elliptical vibration cutting system, (a) Not machining, (b) Machining

2. Elliptical Vibration Cutting Model

Elliptical vibration cutting is a method which synchronizes two-directional vibrations applied to the tool edge in the plane mainly including the cutting direction (bending direction) and the chip flow direction (axial direction) in such a way that the tool edge forms an elliptical locus in each cycle of the vibration. Fig. 1 shows a schematic illustration of the ultrasonic elliptical vibration cutting process. As the maximum vibration speed is set to be higher than the cutting speed, the tool separates from the chip in each cycle of the vibration. The cutting takes place after the re-entrance of the cutting edge into the workpiece, and the chip is mainly pulled up and formed while the tool moves upward in the chip flow direction. The tool moves downward without cutting while it is separated from the chip.[13] That is, the ultrasonic elliptical vibration cutting process can be divided into two parts: cutting part and non-cutting part. In addition, the cutting part can be divided into two cutting processes, i.e. ploughing process and material removing process.

When the tool edge vibrates in two directions, cutting forces are applied to the tool edge as additional periodic forces during machining. These cutting forces can be separated into two components, which are the bending directional cutting force and axial directional cutting force. Fig. 2 shows schematic illustrations of a model of ultrasonic elliptical vibration cutting system when it is (a) not machining and (b) machining. The elliptical vibration cutting system can be described as a two degree of freedom system. According to the position of the tool edge in the elliptical locus, different cutting forces are applied to the tool edge resulting from different cutting processes. In other words, the cutting processes affect the vibration state of the cutting edge and the cutting forces can be represented as additional springs and dampers in the two degree of freedom vibration system. Moreover, these additional dynamic parameters will be represented as changes of internal data in the ultrasonic elliptical vibration controller, and they are described in Section 3. To estimate the cutting processes from the internal data, understanding of the relation between the cutting forces and the additional dynamic parameters are needed first.

When the tool edge passes through the bottom domain of the elliptical locus (when the velocity of bending vibration is the maximum and the position in the axial direction is the maximum toward the cut surface side, as shown by t_1 to t_c in Fig. 3), the ploughing process acts dominantly against the tool edge. Two components of the cutting force are applied to the tool edge, which are the frictional force between the cut surface and flank face and the normal force from the cut surface to the flank face, as shown by F_{bp} and F_{ap} in Fig. 3(a) respectively.

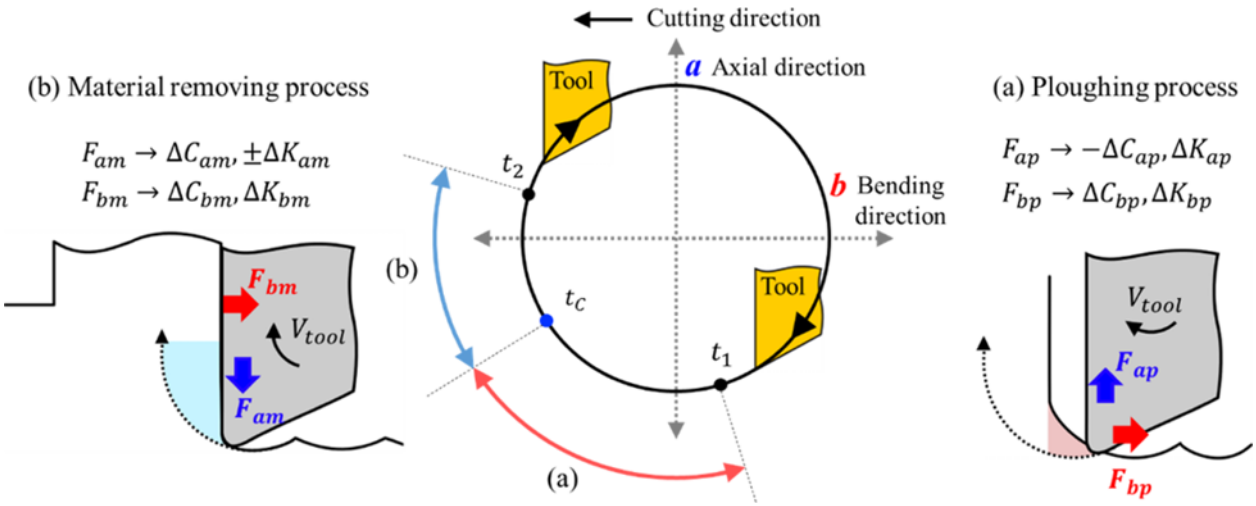

Fig. 3 Cutting processes, (a) Ploughing process and (b) Material removing process

Assume that ΔC_{bp}, ΔC_{ap}, ΔK_{bp} and ΔK_{ap} are the additional equivalent damping and spring coefficients in the bending vibration and axial vibration directions respectively which are caused by the ploughing process. During the ploughing process, the directions of F_{bp} and velocity of bending vibration are opposite, so that ΔC_{bp} acts positively to the vibration system which means more frictional or damping energy is consumed. However, the directions of F_{ap} and axial vibration are the same in most of the ploughing process (they are opposite only in the early moment of ploughing) so that ΔC_{ap} acts negatively to the vibration system which means energy can be saved if the vibrational state is constant. In addition, because the position of the tool edge is the maximum toward the cut surface and F_{ap} acts in the opposite direction to it, ΔK_{ap} acts positively to the vibration system which means stiffness of the axial vibration increases.

On the other hand, the material removing process occurs from the end of the ploughing process to when the velocity of the tool edge towards the cutting direction becomes zero (as shown by t_c to t_2 in Fig. 3). Therefore, the material removing process is mainly applied to the tool edge when the velocity of axial vibration is the maximum and the tool edge's position in the bending direction is the maximum toward the chip side. The workpiece material is sheared and removed as a chip, while the tool moves mainly upward in the chip flow direction in the elliptical vibration cutting. Moreover, the axial vibration speed is larger than the chip flow speed so that frictional force between the chip and rake face of the tool becomes reversed (shown by F_{am} in Fig. 3(b)) and the tool can pull up the chip in this process. F_{am} is applied to the axial vibration mode and a restoring force from the chip to the tool (shown by F_{bm} in Fig. 3(b)) is applied to the bending vibration in the material removing process. ΔC_{am}, ΔC_{bm}, ΔK_{am} and ΔK_{bm} are the additional equivalent damping and spring coefficients in the axial and bending vibration directions respectively which are caused by the material removing process.

During the material removing process, the direction of F_{am} is opposite compared to that of the ploughing process, hence ΔC_{am} acts positively to the vibration system which means more frictional or damping energy is consumed. Regarding to the additional equivalent spring coefficient in the axial vibration, it can be either positive or negative because the tool edge passes the center of the axial vibration. ΔK_{am} acts positively to the vibration system before the center, while it acts negatively after the center. It depends on the cutting and vibration conditions.

As a result, ΔC_a, ΔC_b, ΔK_a and ΔK_b in the model of ultrasonic elliptical vibration cutting system as shown in Fig. 2(b) can be represented as follows.

$$\Delta C_a = -\Delta C_{ap} + \Delta C_{am} \tag{1}$$

$$\Delta C_b = \Delta C_{bp} + \Delta C_{bm} \tag{2}$$

$$\Delta K_a = \Delta K_{ap} \pm \Delta K_{am} \tag{3}$$

$$\Delta K_b = \Delta K_{bp} + \Delta K_{bm} \tag{4}$$

3. Internal Data of Vibration Device for Process Monitoring

The ultrasonic elliptical vibration device consists of an elliptical vibration tool and its controller. The vibration tool utilizes two piezoelectric actuators to excite the two directional resonant vibration modes which are the 1st mode of axial vibration and the 3rd mode of bending vibration. In order to keep large vibration amplitudes during the machining, a constant alternating voltage having the same frequency as the resonant frequency of the axial mode in this device should be applied to the piezoelectric actuators.[14] However, according to the conditions of cutting load or tool wear, the resonant frequency of the axial mode changes slightly. Therefore, the controller chases the resonant frequency of the axial mode by using a system called Phase Lock Loop (PLL), see Fig. 4. Two different voltages, which have a phase difference between them, are applied to the two piezoelectric actuators, and the actuators excite the axial and bending vibration modes. The piezoelectric actuator *a* excites the axial mode, while the actuator *b* excites the bending mode.

When cutting the material with this vibration tool, the energy

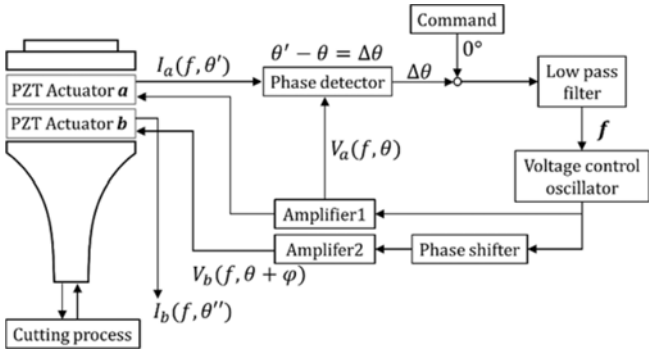

Fig. 4 Block diagram of ultrasonic elliptical vibration control system

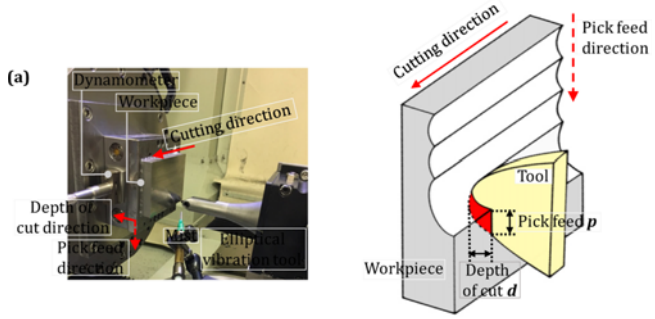

Fig. 5 Experimental method, (a) Photograph of experimental setup and (b) Schematic illustration of cutting process

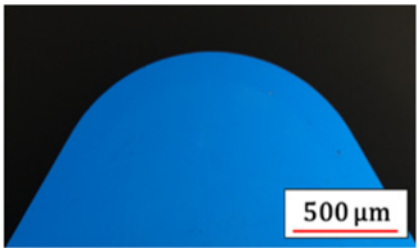

Fig. 6 Microphotograph of rake face of single crystalline diamond tool

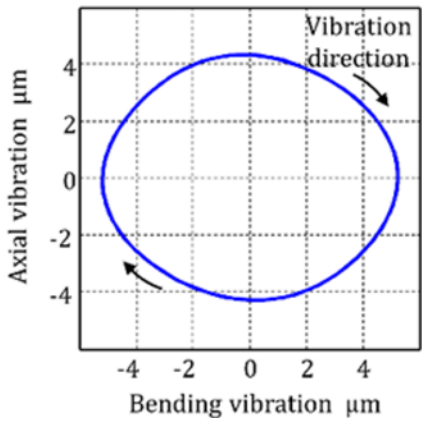

Fig. 7 Measured locus of utilized elliptical vibration

(dynamic) state of the vibration tool will be changed because of the cutting forces. According to the states of the vibration tool, the amplitudes or phases of the electric currents (shown by I_a, I_b, θ', θ'' in Fig. 4) will change. Especially, as the vibration is in the resonant mode, which means that the frequency of the excited voltage is the same with the resonant frequency, the phase difference $\Delta\theta$ between the excited voltage and electric current is zero. Therefore, to chase the resonant frequency of the axial mode, the PLL is configured in order to make the phase difference $\Delta\theta$ between the excited voltage and electric current flowing in the piezoelectric actuator for the excitation of the axial mode to be zero continuously. The voltages V_a and V_b applied to the piezoelectric actuators composing the device, the electric currents I_a and I_b flowing through the actuators, and the excitation frequency f are utilized as the internal data for process monitoring in the proposed method.

Changes of electric powers ΔP_a and ΔP_b, which can be given as products of the voltages and the currents for both piezoelectric actuators, should correlate with the additional damping elements ΔC_a and ΔC_b in Fig. 2(b) which are mainly caused from the frictional force F_{am} between the chip and rake face of the tool due to the material removing process and the frictional force F_{bp} between the cut surface and flank face of the tool due to the ploughing process respectively. This is because these frictional forces make the vibration tool to consume the vibration energy, and they are applied when the vibration tool moves with the maximum velocities of each vibration so that they will act as dampers in the vibration model.

On the other hand, the change of the elliptical vibration frequency Δf_a, which is the resonant frequency of the axial mode, should correlate mainly with the additional spring ΔK_a due to the cutting processes. This is because the resonant frequency is determined by the state of the vibration system, especially the spring coefficient and it can be indicated by Eq. (5).

$$f = \frac{1}{2\pi}\sqrt{\frac{K}{M}} \tag{5}$$

Here, M and K are the total equivalent mass and spring coefficients of vibration system respectively.

Therefore, if the tool wear increases which results in the increased normal force F_{ap} from the cut surface to tool edge, the additional spring coefficient ΔK_{ap} will increase and hence the change of elliptical vibration frequency Δf_a will increase.

4. Methods for Experiments and Evaluation

4.1 Fundamental Cutting Experiments

Fundamental cutting experiments are carried out in order to investigate the correlation between the elliptical vibration cutting process and internal data in the elliptical vibration controller. The machining load is varied with the depth of cut and pick feed, which means different ploughing process and different material removing process occur. In this paper, although the machining load is determined by the depth of cut and pick feed, results of experiments are explained with the cutting width and average uncut chip thickness. This is because the cutting width is related to both the ploughing process and material removing process, while the average uncut chip thickness is mainly related to the material removing process in the elliptical

Table 1 Experimental conditions

Workpiece	Material: Hardened die steel (Stavax)
	Hardness: 54 HRC
Tool	Single crystalline diamond tool
	Rake angle: 0°
	Flank angle: 10°
	Nose radius R: 0.8 mm
Vibration conditions	Frequency: 17.69 kHz
	Amplitude in bending direction: 10 μm_{p-p}
	Amplitude in axial direction: 8.5 μm_{p-p}
Cutting conditions	Depth of cut d (mm): 0.05 / 0.1 / 0.2
	Pick feed p (mm): 0.005-0.18
	Cutting speed: 1000 mm/min
	Cutting fluid: Oil mist

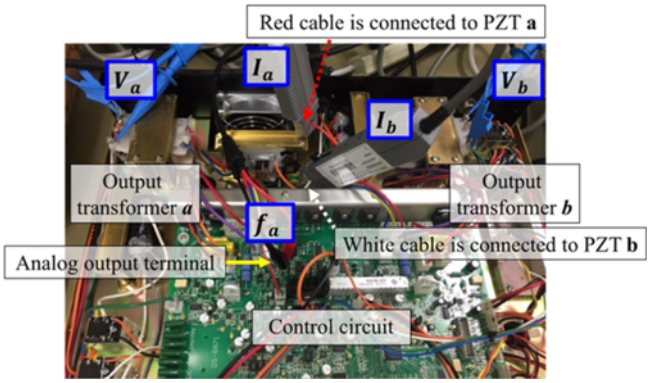

Fig. 8 Photograph of measurement setup

vibration cutting process. In this paper, the cutting width w and average uncut chip thickness t are calculated as follows.

$$w = R\cos^{-1}\left(\frac{R-d}{R}\right) \tag{6}$$

$$t = \frac{pd}{w} \tag{7}$$

Here, R is the nose radius of the tool tip, and d and p are the depth of cut and pick feed respectively.

The cutting experiments are carried out on an ultraprecision machine tool (Fujikoshi, NANO ASPHER ASP01UPX) equipped with an elliptical vibration tool. Fig. 5 shows a photograph of the experimental setup and a schematic illustration of the cutting process. The cutting process is a three-dimensional cutting using the nose of the single crystalline diamond tool. Fig. 6 shows a microphotograph of the rake face of the single crystalline diamond tool taken before the experiments. Fig. 7 shows the locus of the elliptical vibration measured at the tool tip with laser Doppler vibrometers (Graphtec Corp., AT3700-AT0042). It shows that the elliptical vibration tool generates the elliptical vibration with amplitudes of about 10 μm_{p-p} in the bending direction and 8.5 μm_{p-p} in the axial direction at 17.69 kHz, which corresponds to the maximum vibration speed of 33.2 m/min and 28.1 m/min respectively. A typical hardened die steel of Stavax (AISI 420 modified) with hardness of 54 HRC is used as the workpiece material, and it is fixed on a dynamometer (Kistler, 9256C) to measure cutting forces as data for reference of the cutting process. Oil mist is supplied to the cutting point during the machining. The experimental conditions are summarized in Table 1.

4.2 Experimental Setup for Mirror Surface Finishing of Hardened Die Steel with a Single Crystalline Diamond Tool

Considering the utilization of the proposed monitoring method, mirror surface finishing of hardened die steel with a single crystalline diamond (SCD) tool, which is the most common application of the elliptical vibration cutting method, is carried out. This experiment is carried out on the same precision machining tool and elliptical vibration tool as the previous experiments (Section 4.1), but the pick feed is restrained to 0.02 mm for obtaining a mirror surface. The depth of cut is also fixed to be 0.1 mm. The experiments are continued until the total cutting distance becomes more than 900 m, and in this series of the machining experiments the tool wear is observed at some cutting distances with a measuring microscope (Nikon, MM-40/L3U). It is expected that the tool wear will increase as the cutting distance becomes longer, which means that the effect of the cutting edge condition on the internal data will be clarified.

4.3 Analytical Method for Internal Data

During the experiments mentioned above in Sections 4.1 and 4.2, the internal data of the controller, i.e. voltages, currents, and vibration frequency signal, are measured. Fig. 8 shows a photograph of measurement setup of the ultrasonic elliptical vibration controller. Two current probes (Yokogawa, 701933) and two passive probes (Yokogawa, 700929) are utilized to measure the currents and voltages, respectively. After the experiment, the analysis of the measured data is conducted by MATLAB for calculating the power consumption and resonant frequency.

Fig. 9 shows an example of the measured internal data, and Figs. 9(b) and 9(c) correspond to the data before machining and during machining respectively. As shown in Figs. 9(a) to 9(c), amplitudes or phases of currents change during the machining. However, the amplitudes of applied voltages are maintained constantly, while the oscillated frequency is changed slightly. This frequency is the same as the resonant frequency for the chased axial vibration mode.

The average electric powers during a certain period T before machining and during machining can be calculated by determining the sum of products of the electric voltages and currents, and it can be expressed as follows. In this research, T is set as 3 seconds.

$$P_{a\ or\ b} = \frac{1}{T}\int_{t_{st}}^{t_{st}+T} V_{a\ or\ b}(t) \times I_{a\ or\ b}(t)dt \tag{8}$$

The elliptical vibration frequency can be identified by using the vibration frequency signal. It has a square wave form with a constant voltage of 12 V and the fast Fourier transform (FFT) can be used to compute the frequency of the signal. Fig. 10 shows the FFT results of the vibration frequency signals before (from 1 sec to 4 sec in Fig. 9(a)) and during the machining (from 5.5 sec to 8.5 sec in Fig. 9(a)). As shown in Fig. 10, the peak of the graph is shifted to a larger frequency during the machining, which means that the resonant frequency of the axial mode increases because of the elliptical vibration cutting process.

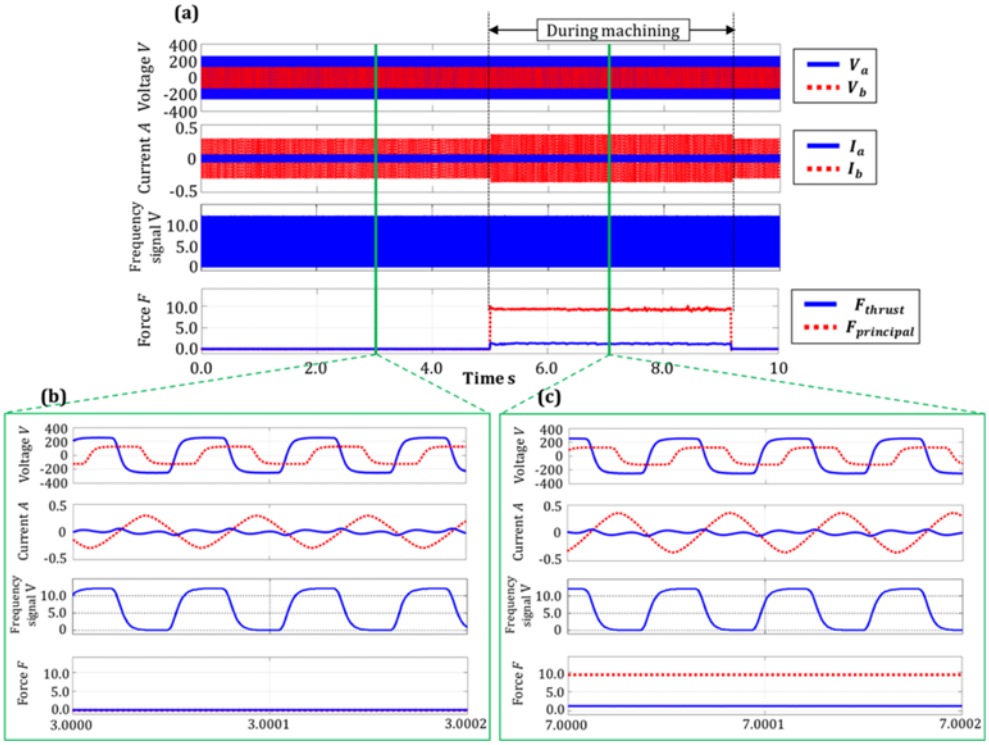

Fig. 9 Measured voltages, currents, vibration frequency signal, and cutting forces (Experiment results in Section 4.1_workpiece: Hardened die steel, tool : Single crystalline diamond tool, cutting speed: 1000 mm/min, depth of cut: 0.2 mm, pick feed: 0.07 mm) (a) Graph of measured internal data and cutting forces, (b) Magnified graph of measured internal data and cutting forces before machining, and (c) Magnified graph of measured internal data and cutting forces during machining

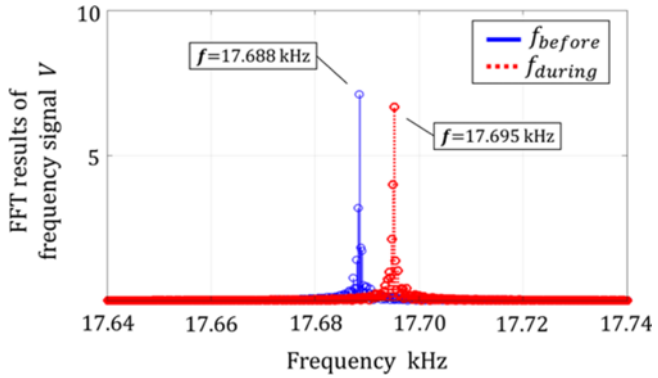

Fig. 10 FFT results of vibration frequency signals before machining and during machining (Experimental results in Section 4.1 workpiece: Hardened die steel, tool: Single crystalline diamond tool, cutting speed: 1000 mm/min, depth of cut: 0.2 mm, pick feed: 0.07 mm)

5. Results and Discussions

5.1 Results and Discussions of Fundamental Cutting Experiments

Fig. 11 shows the cutting forces measured during the machining. The principal force increases as the uncut chip thickness and the cutting width increase. When they increase, the area of cross section of the uncut chip increases and it results in the increased shearing force to remove the material and the increased principal force. The thrust force increases until the uncut chip thickness reaches 0.01 mm. The thrust force is different according to the cutting width. The increased thrust force means that the ploughing process becomes stronger. However, when the uncut chip thickness is larger than 0.01 mm, the thrust forces decrease. This can be explained by the chip-pulling effect of the material removing process as explained in Section 2. When the uncut chip thickness increases, the contact area between the chip and rake face of the tool also increases, and it results in an increase of the chip-pulling force. This means that there is a reversed frictional force applied between the chip and rake face during the material removing process, so that it leads to the decreased thrust force.

The internal data, i.e. change of power consumption for the axial vibration ΔP_a and change of power consumption for the bending vibration ΔP_b are plotted in Figs. 12 and 13 respectively.

As shown in Fig. 12(a), the change of power consumption for the axial vibration ΔP_a increases with the increase of the uncut chip thickness. This is because of the increased chip-pulling force or reversed friction which acts as an additional damping for the axial mode (shown by ΔC_{am} in Fig. 3). As a result, more power is required to maintain the constant vibration states. Meanwhile, when the uncut chip thickness is smaller than about 0.007 mm (Fig. 12(b)), the power consumption for axial vibration is smaller than zero. This also corresponds to the vibration model of elliptical vibration cutting process. When the thickness is small, the ploughing process affects dominantly so that F_{ap} mainly works in the axial vibration direction. According to the phase relationship between F_{ap} and velocity of the axial vibration, the force acts as an additional negative damping to the axial vibration (shown by $-\Delta C_{ap}$ in Fig. 3). As a result, less power is required to maintain the constant vibration states.

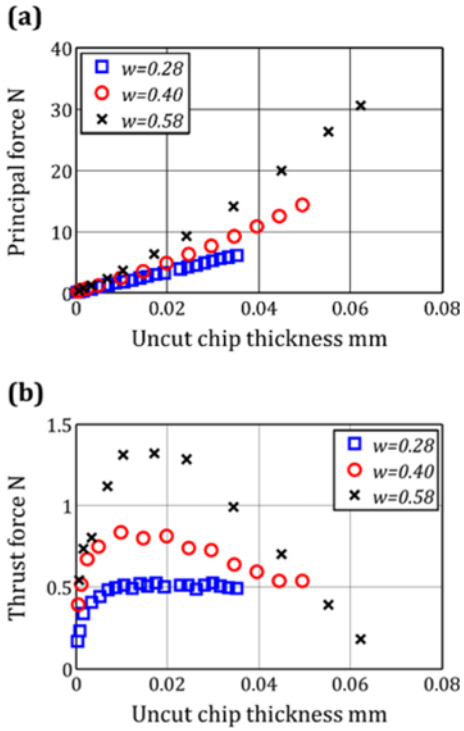

Fig. 11 Measured cutting forces, (a) Principal and (b) Thrust

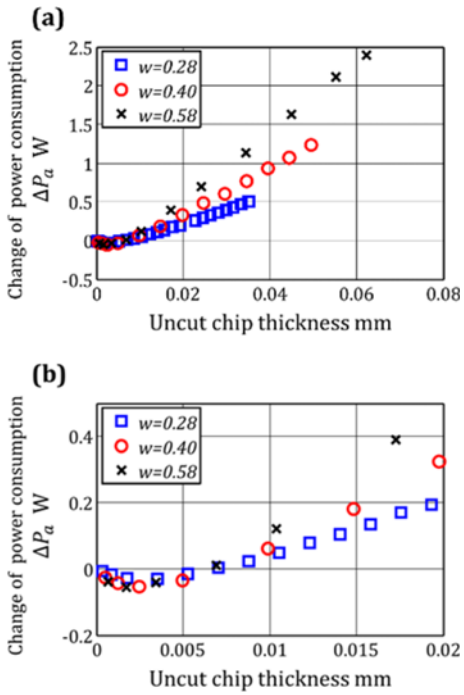

Fig. 12 Change of power for axial vibration, (a) Results at the all cutting conditions and (b) Magnified graph in the range from 0 mm to 0.02 mm

Fig. 13 indicates the change of power consumption for the bending vibration ΔP_b. As shown in Fig. 13, ΔP_b increases radically with the increase of uncut chip thickness until the uncut chip thickness reaches about 0.01 mm. However, its inclination relaxes after 0.01 mm. This can be considered as the magnitude difference between the damping

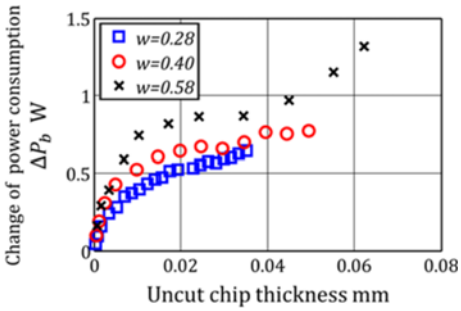

Fig. 13 Change of power for bending vibration

coefficients for the bending vibration caused by the ploughing process and the material removing process (shown by ΔC_{bp} and ΔC_{bm} in Fig. 3). When the cutting edge engages the workpiece in the ploughing process, it moves with a higher velocity for the bending vibration direction compared with when the cutting edge engages in the material removing process. When the bending directional velocity is higher (corresponding with the ploughing process), the consumed energy increases because of the increased velocity. It means that ΔC_{bp} is larger than ΔC_{bm}. As a result, the inclination of the change of power consumption in the bending vibration is also large when the uncut chip thickness is in a range from 0 mm to 0.01 mm. However, when the chip thickness is large, the effect of the ploughing process will not change so much. Therefore, the inclination of the change of power consumption in the bending vibration is small. When the uncut chip thickness is around 0.06 mm, the inclination increases again, and this can be explained by the increase of ΔC_{bm}.

Fig. 14 shows the phase of admittances calculated from the applied voltages (shown by V_a, V_b in Fig. 4) and currents (shown by I_a, I_b in Fig. 4) flowing through the piezoelectric actuators *a* and *b*.

As shown by "*be-axial*" in Fig. 14, the phases of admittance of piezoelectric actuator *a* before the machining are -40 deg, but it should be 0 deg because the elliptical vibration controller chases the resonant frequency of the axial vibration as explained in Section 3. The reason can be considered as follows. At first, the elliptical vibration controller used in this research adopts switching amplifiers, hence I_a contains harmonic components of the excitation frequency. This results in the deformed waveform of I_a as shown in Figs. 9(b) to 9(c). Moreover, because the controller chases the anti-resonance with the alternative voltage which has a constant magnitude, the magnitude of current is the minimum. These facts lead to an error in the phase detector (see Fig. 4) detecting the phase differences between V_a and I_a with the zero-crossing method.

However, note that the magnitude of admittance at the anti-resonance is an inflection point, and the phase is changed from -90 deg to 90 deg before and after the resonant frequency, which is a change that happens too drastically. Therefore, even though the phase differences are -40 deg, it still can be concluded that the PLL control system chases the resonant frequency of the axial vibration in a way.

As shown in Fig. 14, the phases of admittance of piezoelectric actuator *a* during the machining (shown by "*du-axial*") change compared to the results of those before the machining, and these differences change against the machining load, too. In addition, the

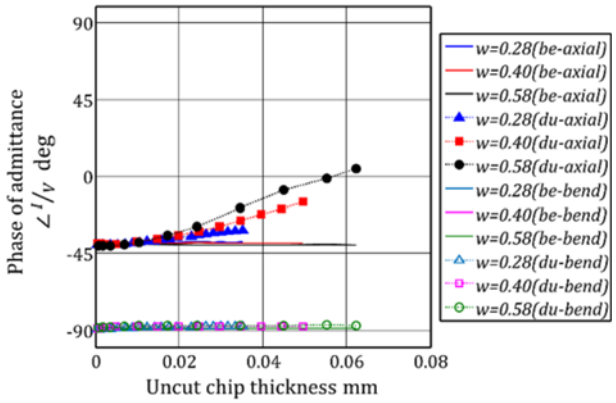

Fig. 14 Phases of admittance

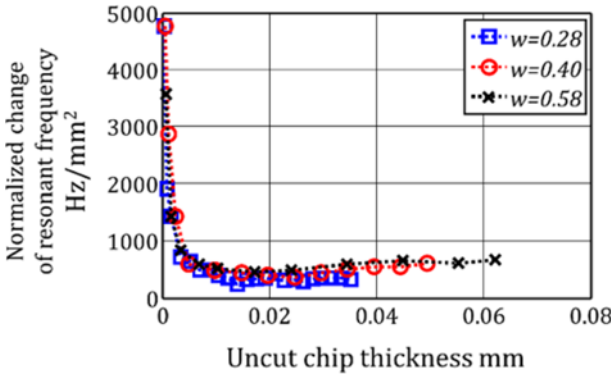

Fig. 15 Normalized change of resonant frequency of axial vibration mode against uncut chip thickness

magnitude of V_a and I_a do not change as shown in Fig. 9(a). This implies that the changes of power consumption ΔP_a against the change of machining load are caused by the change of phase differences rather than the change of the magnitude of the current.

Meanwhile, as shown by "*be-bend*" and "*du-bend*" in Fig. 14, the phases of admittance at the piezoelectric actuator *b* before and during the machining do not change compared to the results of axial vibration. The values are about -90 deg. This indicates that the resonant frequency of the bending vibration is slightly larger than that of the axial vibration. As shown in Fig. 9(a), the magnitude of the current I_b changes during the machining. This implies that the changes of power consumption ΔP_b against the change of machining load are caused by the change of the magnitude of the current rather than the change of phase differences.

As mentioned in Section 4.1, the cutting width affects the material removing process and ploughing process, and the average uncut chip thickness affects the material removing process during the machining. Therefore, it is difficult to distinguish the effect of each process on the stiffness or resonant frequency of the vibration system. In this research, a normalization of the change of resonant frequency of the axial vibration Δf_a is carried out to distinguish them. Fig. 15 shows the normalized change of resonant frequency of the axial vibration mode against uncut chip thickness. The results are calculated from the change of resonant frequency of the axial vibration mode divided by the area of cross section of the uncut chip. As shown in Fig. 15, when the uncut chip thickness is small, i.e. ploughing process occurs mainly, the normalized results are larger compared to those of when the uncut chip thickness is large. It implies that ΔK_{ap} is larger than ΔK_{am}, and this corresponds to the proposed model. It is because the position of the cutting edge is the maximum in the axial vibration during the ploughing process, while it is around the center of the axial vibration during the material removing process. Therefore, it can be concluded that the change of resonant frequency of the axial vibration mode is mainly affected by the ploughing process.

However, as mentioned in the discussion of the phase difference, the chasing of resonant frequency of the axial mode is not accurate. Therefore, it is considered that the reliability of the resonant frequency data is relatively lower to monitor the cutting process than the other internal data.

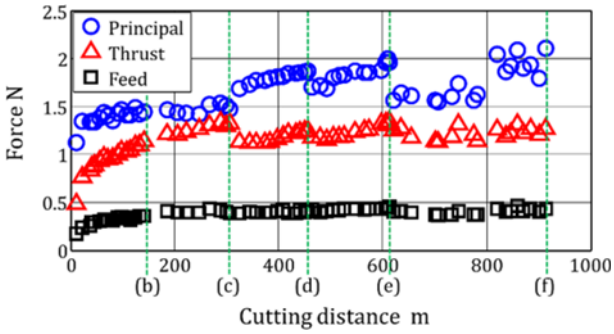

Fig. 16 Measured cutting forces against cutting distance

5.2 Results of Mirror Surface Finishing

The cutting forces measured during the experiment mentioned in Section 4.2 are plotted against the cutting distance in Fig. 16. Although the change of the cutting forces is discontinuous because the tool wear observations are carried out at some cutting distances, all components increase gradually as the machining progresses. This is because the tool is worn according to the cutting distance, so that the sharp cutting tool edge at the beginning becomes dull gradually. In the ordinary cutting method, it is hard to machine hardened steel with a diamond tool because of its rapid tool wear. However, in the elliptical vibration cutting, the tool wear of diamond tool is drastically decreased because of its unique characteristic, i.e. intermittent cutting.[15,16]

The moments where the tool observations are carried out are marked by green dashed lines in Fig. 16, and they correspond with Figs. 16(b) to 16(f).

Fig. 17(a) indicates the schematic illustration of the cutting process, and the red area corresponds to the area of cross section of the uncut chip when the cutting condition is set as depth of cut *d* and pick feed *p*. Figs. 17(b) to 17(f) show the photographs of the rake face of the tool, and this supports the fact that the tool wear progresses gradually and continuously. As shown in Fig. 17, the tool wear is different along the cutting edge. Where the uncut cut chip thickness is small, a small tool wear is observed even though the cutting distance is more than 900 m. This position of the tool mainly engages for finishing the mirror surface

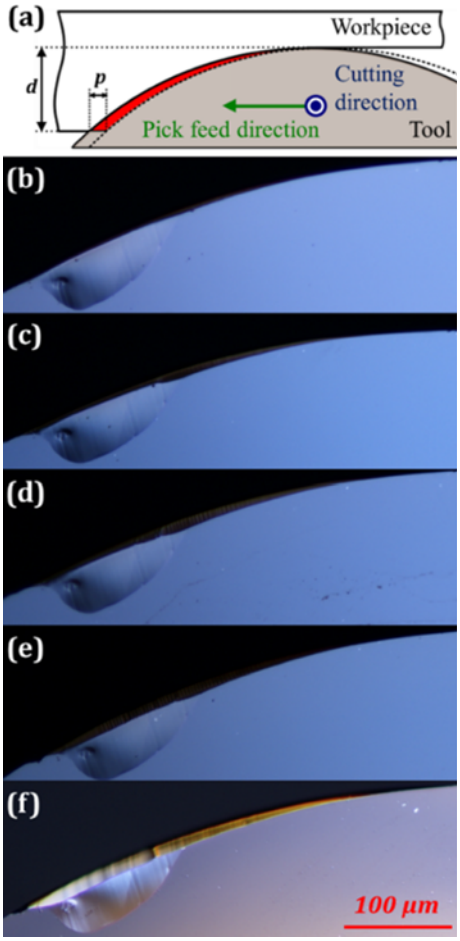

Fig. 17 Tool wear observation, (a) Schematic illustration of uncut chip and Microphotographs of rake face when the cutting distance is (b) 141 m, (c) 305 m, (d) 456 m, (e) 612 m, and (f) 914 m

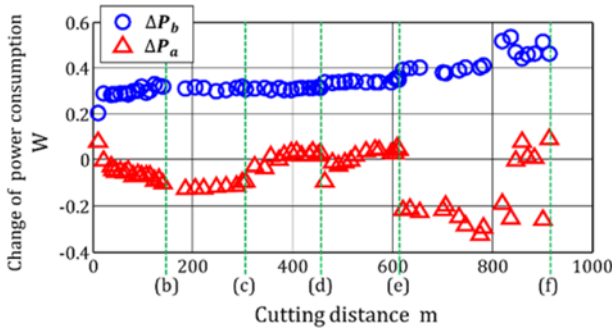

Fig. 18 Change of power consumption

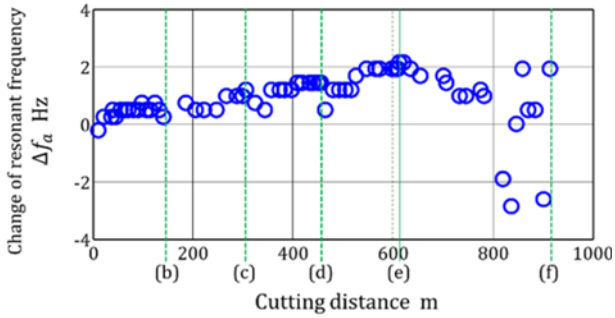

Fig. 19 Change of resonant frequency of axial vibration mode against cutting distance

so that a high quality mirror surface can be obtained although tool wear is observed in a different position of the cutting edge.[14]

Fig. 18 shows the changes of power consumptions for axial vibration and bending vibration during the experiment. ΔP_b gradually increases as the cutting distance increases. Affected by the tool wear, the roundness of the cutting edge becomes larger, and the frictional force between the cut surface and cutting edge increases in the ploughing process (shown by F_{bp} in Fig. 3). F_{bp} acts as an additional damping for the bending mode (shown by ΔC_{bp} in Fig. 3). Moreover, the change of ΔP_b correlates well with the change of the principal force shown in Fig. 16. The cutting conditions are constant in this experiment, so it can be concluded that the increase of the principal force is caused by the tool wear which is indicated in the change of ΔP_b.

Compared to ΔP_b, ΔP_a generally decreases during the experiment. Considering the cutting condition, the average uncut chip thickness is about 0.007 mm. Because of its small uncut chip thickness, the effect of the chip-pulling process is minor. This is also indicated by the positively increased thrust force in Fig. 16.

When the chip-pulling process is minor, the frictional force between the chip and rake face does not act dominantly as an additional damping for the axial mode (shown by ΔC_{am} in Fig. 3). Instead, the force resulting from the ploughing process acts as a negative damping and a positive spring (shown by $-\Delta C_{ap}$, ΔK_{ap} in Fig. 3). As a result, the change of the power consumption for axial vibration decreases (Fig. 18) and the change of resonant frequency for axial vibration increases (Fig. 19).

6. Conclusion

Monitoring of ultrasonic elliptical vibration cutting process by utilizing internal data in the ultrasonic elliptical vibration device without utilizing external sensors such as a dynamometer and displacement sensor is investigated. The internal data of the ultrasonic elliptical vibration device, i.e. voltages applied to the piezoelectric actuators composing the device, electric currents flowing through the actuators, and resonant frequency of the axial vibration mode chased by PLL, were measured before and during machining under various conditions. Through several experiments of diamond cutting of hardened die steel experiments, the following conclusions can be drawn.

(1) The internal data changes according to the states of the cutting process. By calculating the changes of the internal data between before the machining and during the machining, it is possible to estimate the cutting process.

(2) When the average uncut chip thickness is small, the change of

power consumption for axial vibration is smaller than zero or decreases. This corresponds to the increase of the thrust force. However, the power consumption increases when the uncut chip thickness is large because of the increased material removing process. This corresponds to the decrease of thrust force. When the tool wear progresses, the power consumption for the axial vibration decreases gradually because of the decreased chip pulling effect and increased ploughing process.

(3) When the average uncut chip thickness is small, the change of power consumption for the bending vibration increases with a large inclination against the uncut chip thickness because of the increased ploughing process. However, its inclination decreases when the uncut chip thickness is large. This is because when the uncut chip thickness is large, the ploughing process does not change so much against the uncut chip thickness. Therefore, the effect of material removing process on the equivalent damping of bending vibration is smaller than that of the ploughing process. Moreover, when the tool wear progresses, the change of power consumption for the bending vibration increases because of the increased ploughing process.

(4) When the cutting width increases and the tool wear progresses, the change of resonant frequency for the axial vibration increases because the increased ploughing process yields a larger additional spring. However, it has a low reliability compared to the other internal data. This is because the resonance chasing of axial vibration mode is not accurate. The chasing error is caused by the switching amplifier which generates the harmonic components of the current and hence leads to an error of the phase detection.

As a result, it is clarified that the internal data, i.e. the changes of power consumption in each vibration, correlates well with the machining process. The correlations agree with the proposed model, and hence it is expected that the internal data can be utilized to realize the proposed monitoring of the elliptical vibration cutting process, such as tool wear and sudden change of machining load.

ACKNOWLEDGEMENT

The authors would like to thank the Graduate program for Real-World Data Circulation Leaders in Nagoya University and Research Fellow of Japan Society for the Promotion of Science (DC1) for financial supports and the TAGA electric for technical support.

REFERENCES

1. Kang, H. S., Lee, J. Y., Choi, S., Kim, H., Park, J. H., et al., “Smart Manufacturing: Past Research, Present Findings, and Future Directions,” International Journal of Precision Engineering and Manufacturing-Green Technology, Vol. 3, No. 1, pp. 111-128, 2016.
2. Park, S.-J., Lee, H.-S., and Jeong, H., “Signal Analysis of CMP Process Based on AE Monitoring System,” International Journal of Precision Engineering and Manufacturing-Green Technology, Vol. 2, No. 1, pp. 15-19, 2015.
3. Chua, Z. Y., Ahn, I. H., and Moon, S. K., “Process Monitoring and Inspection Systems in Metal Additive Manufacturing: Status and Applications,” International Journal of Precision Engineering and Manufacturing-Green Technology, Vol. 4, No. 2, pp. 235-245, 2017.
4. Delio, T., Tlusty, J., and Smith, S., “Use of Audio Signals for Chatter Detection and Control,” Journal of Engineering for Industry, Vol. 114, No. 2, pp. 146-157, 1992.
5. Smith, S. and Tlusty, J., “Stabilizing Chatter by Automatic Spindle Speed Regulation,” CIRP Annals-Manufacturing Technology, Vol. 41, No. 1, pp. 433-436, 1992.
6. Altintas, Y., “Prediction of Cutting Forces and Tool Breakage in Milling from Feed Drive Current Measurements,” ASME Journal of Engineering for Industry, Vol. 114, No. 4, pp. 386-392, 1992.
7. Stein, J. L. and Huh, K., “Monitoring Cutting Forces in Turning: A Model-Based Approach,” Journal of Manufacturing Science and Engineering, Vol. 124, No. 1, pp. 26-31, 2002.
8. Kakinuma, Y. and Kamigochi, T., “External Sensor-Less Tool Contact Detection by Cutting Force Observer,” Procedia CIRP, Vol. 2, pp. 44-48, 2012.
9. Jiang, C., Zhang, Y., and Xu, H., “In-Process Monitoring of Tool Wear Stage by the Frequency Band-Energy Method,” CIRP Annals-Manufacturing Technology, Vol. 36, No. 1, pp. 45-48, 1987.
10. de Jesus, R.-T. R., Gilberto, H.-R., Ivan, T.-V., and Carlos, J.-C. J., “Driver Current Analysis for Sensorless Tool Breakage Monitoring of CNC Milling Machines,” International Journal of Machine Tools and Manufacture, Vol. 43, No. 15, pp. 1529-1534, 2003.
11. Rivero, A., de Lacalle, L. L., and Penalva, M. L., “Tool Wear Detection in Dry High-Speed Milling Based Upon the Analysis of Machine Internal Signals,” Mechatronics, Vol. 18, No. 10, pp. 627-633, 2008.
12. Jung, H., Shamoto, E., Chin, H., Anh, N. V., “Monitoring of Elliptical Vibration Cutting Process by Utilizing Internal Data in Ultrasonic Elliptical Vibration Device,” Proc. of Japan Society for Precision Engineering Spring Meeting, pp. 153-154, 2016.
13. Shamoto, E. and Moriwaki, T., “Study on Elliptical Vibration Cutting,” CIRP Annals-Manufacturing Technology, Vol. 43, No. 1, pp. 35-38, 1994.
14. Shamoto, E., Suzuki, N., Moriwaki, T., and Naoi, Y., “Development of Ultrasonic Elliptical Vibration Controller for Elliptical Vibration Cutting,” CIRP Annals-Manufacturing Technology, Vol. 51, No. 1, pp. 327-330, 2002.
15. Shamoto, E. and Moriwaki, T., “Ultaprecision Diamond Cutting of Hardened Steel by Applying Elliptical Vibration Cutting,” CIRP Annals-Manufacturing Technology, Vol. 48, No. 1, pp. 441-444, 1999.
16. Jung, H., Shamoto, E., Ueyama, T., Hamada, S., and Xu, L., “Mirror Surface Finishing of Hardened Die Steel by High-Power Ultrasonic Elliptical Vibration Cutting,” Journal of Machine Engineering, Vol. 16, No. 1, pp. 5-14, 2016.

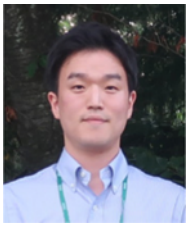

Hongjin Jung
Designated assistant professor in the Department of Aerospace Engineering, Nagoya University. His research interests are in precision machining of difficult-to-cut materials and vibration-assisted cutting.
Email: hongjin.jung@mae.nagoya-u.ac.jp

Takehiro Hayasaka
Assistant professor in the Department of Aerospace Engineering, Nagoya University. His research interest is in metal cutting, especially chatter.
E-mail: takehiro.hayasaka@mae.nagoya-u.ac.jp

Eiji Shamoto
Professor in the Department of Aerospace Engineering, Nagoya University. His research interests are in metal cutting and machine tool.
E-mail: shamoto@nagoya-u.jp